ISSN 1070-3632, Russian Journal of General Chemistry, 2010, Vol. 80, No. 3, pp. 567–575. © Pleiades Publishing, Ltd., 2010.
Original Russian Text © A.V. Agafonov, A.G. Zakharov, 2010, published in Rossiiskii Khimicheskii Zhurnal, 2010, Vol. 53, No. 2, pp. 15–22.

Electrorheological Fluids

A. V. Agafonov and A. G. Zakharov

Institute of Solution Chemistry, Russian Academy of Sciences, ul. Akademicheskaya 1, Ivanovo, 153045 Russia
e-mail: ava@isc-ras.ru

Received January 10, 2009

Abstract—Advances in one of the most promising fields of the chemistry of smart materials, specifically, electrorheological fluids are considered. The electrorheological effect and the structure and properties of electrorheological fluids are described. Modern views on the nature of the electrorheological effect are considered. The review focuses on the application of nanomaterials as the disperse phases in electrorheological fluids. Recent avances in the sol–gel synthesis of nanostructured colloid systems and the electrorheological characteristics of their based liquid systems are considered. Certain aspects of practical application of electrorheological fluids are presented.

DOI: 10.1134/S1070363210030382

INTRODUCTION

Development of highly efficient electrorheological fluids capable of reversibly varying their viscosity and theoretical research in electrorheology is one of the most promising fields of the chemistry of smart materials. This problem relates to priority directions of materials science, such as synthesis of hybrid organic inorganic materials, sol–gel technology, nanomaterials, and electroconducting polymers.

Stability of electrorheological fluids filled with nanosized electrorheologically active materials is one of the most discussed problems of electrorheology. The passage to a nanosized disperse phase much attenuates the gravitational instability of the disperse system, and the special structural organization of nanoparticles due to hybrid formation with polymers much enhances the aggregative stability of the colloid system. The disperse phase with a reduced particle size possesses a lower abrasiveness, which makes possible development of electrorheological devices with smaller interelectrode gaps and microscopic electromechanical systems. The use of nanomaterials as a packing in electrorheological fluids led to a qualitative breakthrough in reaching high electrorheological effects, thus opening up new possibilities for developing devices whose operating principle is based on this effect.

Let us make a short excursus into the history of electrorheology. The electrorheological effect is a fast reversible change of viscosity of colloid dispersions of certain materials in dielectric liquids (Fig. 1). It was discovered by Winslow in 1947 [1, 2] who studied the effect of electric field on the viscosity on silica gel in kerosene. Later such systems were given the name electrorheological fluids. The solid–liquid transition

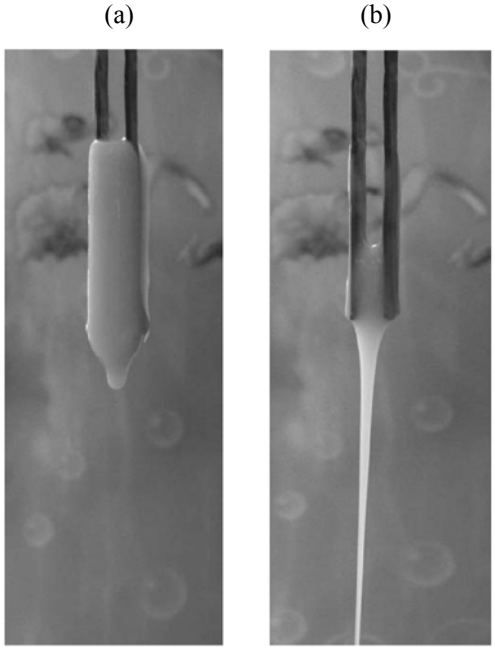

Fig. 1. Demonstration of the electrorheological effect. Electrorheological fluid with the disperse phase (30%) on the basis of a TiO_2–hydroxypropyl cellulose hybrid nanocomposite: (a) fluid in an electric field of 400 V mm^{-1} (interelectrode gap 5 mm) and (b) no electric field is applied.

time in electrorheological fluids is about 1–10 ms. This property created prerequisites for developing electrocontrolled devices realizing the electrorheological effect. The operating principle of such devices is based on the controlled resistance to applied force, created by the electrorheological fluid.

By the end of XX century, hundreds papers and tens of monographs have been published on this issue. At the same time, up to mid-1990s there have been no considerable advances in the development of devices exploiting the electrorheological effect. The principal reason for such a slow progress was the poor efficiency of electrorheological fluids with disperse phases made of natural materials (aluminum silicates and certain biopolymers), and simple oxides.

In the USSR, the electrorheological effect was studied by the Academicians P.A. Rebinder, B.V. Deryagin, A.V. Lykov and their disciples Z.P. Shul'man, E.V. Korobko, Yu.F. Deinega, G.V. Vinogradov, Yu.G. Yanovskii, A.A. Trapeznikov, S.S. Dukhin, V.N. Shilov et al. at the Institute of Physical Chemistry of the Russian Academy of Sciences, Institute of Heat and Mass Exchange of the Belorussian Academy of Sciences, Institute of Colloid and Water Chemistry of the Ukrainian Academy of Sciences, and Laboratory of Polymer Rheology at the Institute of Petrochemical Synthesis of the Academy of Sciences of the USSR. Interesting results were obtained in the research on the mechanism of the electrorheological effect and its dependence on the nature of components of the disperse phase, as well as in the development of devices on the basis of the electrorheological effect [3–7]. The most common disperse phases used in these research works were natural materials (aluminum silicates like vermiculite, diatomite, silica, or titanium dioxide) treated with various activators. After the collapse of the USSR, research in electrorheology in Russia was continued by Yu.G. Yanovskii and his disciples (Institute of Applied Mechanics of the Russian Academy of Scienced, modeling of the electrorheological effect). Devices on the basis of the electrorheological effect are developed at the Bauman Moscow Technical University (Prof. V.P. Mikhailov and Yu.V. Panfilov). In 2005, research on the electrorheological effect and development of electrorheological fluids and devices on their basis were initiated at the Institute of Solution Chemistry of the Russian Academy of Sciences. Note that almost all major foreign universities are involved in R&D in the field of electrorheology, and these activities are funded by automobile, robotic, and aerospace corporations.

Nature of Electrorheological Fluids

Electrorheological fluids are complex colloid systems formed by a dielectric disperse phase with a special structural organization and particle size varying from 10 to 1000 nm, suspended in a dielectric liquid [8–11]. As a rule, liquids with low dielectric constant and electrical conductivity ($\varepsilon \approx 2$, $\sigma < 10^{-15}$ S m^{-1}) are used. The liquid viscosity requirements are determined by the exploitation conditions (high-viscosity liquids are operated at elevated temperatures). A natural requirement is a wide liquid-state range. Electrorheological fluids can contain additives enhancing both the electrorheological effect and sedimentative and aggregative stability. Apart from the above properties, these fluids should exhibit a low abrasiveness and resistance to chemicals, and be nontoxic. The concentration of the disperse phase in practically significant systems varies from 20 to 60% [12].

The main characteristic feature of electrorheological systems is their ability to suffer, under applied electric field, fast (within milliseconds) reversible (in the absence of field the effect disappers) transitions from the liquid state to viscoelastic up to complete loss of fluidity and transition to the solid state. The fact that the physicomechanical characteristics of electrorheological fluids vary in parallel with the electric field strength opens up possibilities for controlling properties of the system, for example, to induce controlled resistance to applied force.

Physical Models of the Electrorheological Effect

The property of disperse systems to enhance viscosity under electric field and pass into the viscoelastic state is underlain by the formation of chain structures. Therewith, initially separate chains are formed in the interelectrode space. As the electric field strengh increases, the chains increase in number, and combine to form packs and then stacks. The strength of interparticle bonds in the resulting structures and interactiton of the latter with electrodes define the physicomechanical properties of electrorheological fluids and the strength of the electrorheological effect [13].

A number of particular approaches and models were suggested to interpret this phenomenon [14–20]. Since interparticle interactions are largely determined by the physicochemical and structural features of the disperse phase particles, of importance are models that

relate the structural and chemical organization of the particle material and the strength of the electrorheological effect.

The mechanism of the interaction of disperse phase particles of electrorheological fluids, leading to viscosity enhancement, according to speculations in [21–23], suggests that the exposure of disperse phase particles containing adsorbed water to electric field gives rise to electroosmosis. The ions contained in material pores start to migrate from pores to particle surface, carrying water with them. The water molecules localize on the surface in the areas with a maximum field strength and form briges between particles. Once the electric field has been lifted, capillary and surface tension forces return the water molecules into pores. This phenomenon correspons to the surfactant brigde model.

The stability and rheological properties of electrorheological fluids are controlled by using surfactant additives. The adsoprtion of surfactants enhances the electrorheological effect by enhancing surface polarization of disperse particles and their bridging [24–28].

The dielectric polarization model explains the electrorheological effect in terms interaction of polarized disperse phase particles. The interparticle interaction forces arise from the dielectric difference between the particles and dielectric medium [29–36]:

$$F = 12\pi\varepsilon_0\varepsilon_m a^2\beta^2E^2, \quad (1)$$

where ε_0 and ε_m are the dielectric constants of a vacuum and the disperse medium, respectively; $\beta = (\varepsilon_p - \varepsilon_m)/(\varepsilon_p + 2\varepsilon_m)$, dielectric difference parameter; ε_p, dielectric constant of particles; and E, electric field strength.

From this in follows that the share stress of an electrorheological fluid is quadratically related to electric field strength, which is really observed in practice [14, 16, 20, 30]. A critical point in this model is that the dielectric difference parameter estimated on the basis of dielectric properties tends to one as ε_p increases, which poses a limit on the strength of the effect. With materials with a fairly high dielectric constant, this makes indistinguishable the interaction forces calculated by Eq. (1).

The Maxwell–Wagner polarization model relates the effect to the polarization arising due to charge accumulation at the interface of heterogeneous dielectrics, when two phases differ from each other in dielectric constant and conductivity. The model takes account of the polarization relaxation time, which is not infrequently close to the response time [37, 38]:

$$t_{MW} = \frac{\varepsilon_p + 2\varepsilon_m}{\sigma_p + 2\sigma_m} \simeq \frac{\varepsilon_p + 2\varepsilon_m}{\sigma_p}, \quad (2)$$

where σ_p is the particle conductivity and σ_m, disperse phase conductivity.

As the field strength increases, the particle and fluid conductivity gets more and more dependent on particle shape and interparticle distance. In cases where the electrorheological behavior is controlled by the nonlinear conuctivity arising on an avalanche-like conductivity growth in a small gap between disperse phase particles at a high field strength [39], different models suggest different variants of local field distribution in the vicinity of particles [40–42]. The particle interaction strength and the applied electric field strength E_0 are related by the following formula [43, 44]:

$$F = 2\pi a^2\varepsilon_0\varepsilon_m E_s E_0, \quad (3)$$

where $E_s = 30[\sigma_p/A\sigma_m(0)]^{0.1}E_m^{0.9}E_0^{0.1}$ is the saturation strength of the local interparticle field; σ_p, particle conductivity; $\sigma_m(0)$, conductivity of the dispersion medium in a low-strength electric field; and A and E_m, material-dependent empirical constants.

Experimental measurements of the interaction strength between two semispheres [45] are nicely consistent with the above concept, and, therewith, the interaction strength is quadratically related to E_0 at low electric fields and linearly related at strong electric fields.

Rheology of Electrorheological Fluids

The viscosity of an electrorheological fluid under applied electric field changes from Newtonian (at a zero field strength) to non-Newtonian plastic. The share stress and rate for a dilute electrorheological are linearly related to each other, except the range when the share stress is a minimum, whose length depends in the nature of the disperse phase and the strength of the electric field. Once a certain transitions point has been reached, the electrorheological fluid behaves as a solid. At shear loads above minimal the fluid flows, and this limiting shear stress is proportional to the share rate. The electrorheological fluid flow can be described by the phenomenological Shvedov–Bingham equation:

$$\tau = \tau_{0,d} + \gamma\eta, \quad (4)$$

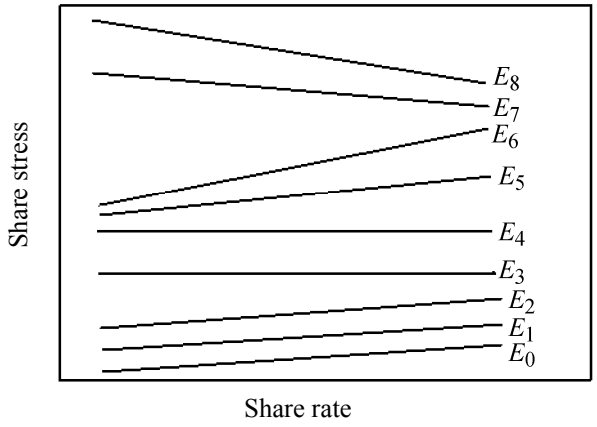

Fig. 2. Example flow curves of electrorheological fluids at varied electric field strengths ($E_0 = 0$, $E_8 > E_7 > E_6 > E_5 > E_4 > E_3 > E_2 > E_1$).

where τ is the share stress; $\tau_{0,d}$, dynamic yield stress depending on the applied electric field strength; γ, share rate; and η plastic, so-called Bingham viscosity.

A general scheme of the dynamic behavior of an electrorheological fluid is shown in Fig. 2.

Electrorheological fluids with a characteristic Bingham behavior (denoted E_0, E_1, E_2 in Fig. 2) are fairly common. The Bingham viscosity of such fluids is, as rule, a constant value. There are systems with a very weak share stress–share rate dependence (denoted E_3 and E_4 in Fig. 2). The Bingham viscosity of such fluids is close to zero. The third group of electrorheological fluids has the share stress increasing with increasing field strength and share rate, and, therewith, the Bingham viscosity also increases with increasing field strength (E_5 and E_6). Certain electrorheological fluids show a phenomenon, when the share stress in electric fields decreases with increasing share rate, and the Bingham viscosity becomes negative (E_7 and E_8). This phenomenon can be associated with the kinetic nature of the electrorheological effect, features of structure formation in electrorheological fluids as a function of disperse phase nature, and presence or absence of adhesive interactions of the fluid with electrode materials in electric fields, as well as with the limited nature of the Shvedov–Bingham model.

In most cases the behavior of electrorheological fluids in electric fields is characterized by more complicated, nonlinear flow curves having maxima and minima. For such systems, exponential models, for example, the Hershel–Barkley model, were suggested [46]:

$$\tau = \tau_{0,d} + k\gamma^n. \quad (5)$$

More sophisticated multiparameter models are also developed [47].

Critical shear stresses of two types are recognized [48]: static yield stress $\tau_{0,s}$ and dynamic yield stress $\tau_{0,d}$. The static yield stress is defined as a stress required to initiate fluid flow, i.e. the solid–fluid transition stress. The dynamic yield stress is a voltage required to induce the fluid-solid transition under a zero shear rate. Such difference arises when a system is exposed to electric field. The static yield stress $\tau_{0,s}$ characterizes a fluid in a quiescent state, subjected first to electric field and then to a share force. The static yield stress can be measured by means of special viscometers with controlled applied force [49]. Differently, field can be applied on a system already subjected to corresponding shear stress, i.e. the fluid flowed before the outer field had been applied; in this case, a characteristic is the dynamic yield stress $\tau_{0,d}$. The dynamic yield stress is calculated by Eqs. (4) and (5) from the flow curves of electrorheological fluids in electric fields. Shift voltages are measured by means of rotation voscometers modified to allow electric field to be appied to the interelectrode gap [50–52]. The static yield stresses of electrorheological liquids are generally higher than dynamic. This phenomenon is called the static friction or stiction which is strongly dependent on the size and shape of disperse phase particles.

The electric field–induced yield stress depends on electric field strength. If the fluid flow under electric field adheres the Shvedov–Bingham equation, the dynamic yield stress increases quadratically with electric field strength [8]:

$$\tau_{0,d} = \alpha E^2.$$

The plastic viscosity is related to field strength by the equation

$$\eta = \eta_0 + C_d E^2,$$

where the coefficient C_d depends on the nature of the electrorheological fluid and can take positive, negative, or zero values according to the flow curves (see Fig. 2).

The static yield stress at low field strengths only slightly differs from that in the absence of field, and, after a certain threshold E_{ref} has been reached, it varies linearly with field strength:

$$\tau_{0,s} = C_s(E - E_{ref}).$$

It should be noted that the equation relating static yield stress to field strength is valid only at field

strengths higher than E_{ref}. Generally, the fact that $\tau_{0,d}$ and $\tau_{0,s}$ differ in physical meaning should be taken into account both in developing the theory of the electrorheological effect and in calculating devices based on this effect.

Effect of the Nature and Structure of the Disperse Matter on the Electrorheological Effect

At the first steps of the development of electrorheology natural materials modified to enhance the electrorheological effect were the most common disperse phases of electrorheological fluids. With the accumulation of knowledge in this field, the role of disperse phase acquired decisive importance. Such substances as fullerenes [53], high-temperature superconductors [54], semiconductor polymers, including polyaniline [55], polypyrroles [56], and co-polyanilines [57], as well as polysaccharides, specifically cellulose phosphates [58], were tested as components of electrorheological fluids at different stages of research in electrorheology. Synthesis of electrorheological nanocomposites using semiconductior polymers as organic components and metal oxides, porous and layered zeolite-like nanostructures, or clays as inorganic components was found to be quite a promising approach. This approach allowed making use of a synergistic effect associated with uniquie properties of polymers encapsulated in an inorganic nanomatrix.

The electrorheological behavior of semiconductor polypyrroles and polypyrrole–inorganic nanocomposited was considered in [59–61]. Sterically stabilized polypyrrole–SiO_2–methyl cellulose and polypyrrole–SnO_2–methyl cellulose nanocomposites were obtained by the polymerization of pyrrole in the presence of an oxidant at various ratios of other components. It was shown that methyl cellulose enhances the electrorheological effect. The dynamic yield stress of dispersions of polypyrrole–SiO_2–methyl cellulose powders in silicone oil (10 vol %) is 1.7 kPa at E = 2 kV mm^{-1}. Pyrrole intercalates obtained by the polymerization of pyrrole directly in clay layer nanoreactors [62] show a strong nonlinear electrorheological response. Electrorheological systems with the disperse phase of propylene glycol–SiO_2 organic–inorganic nanocomposites have a several times higher dynamic yield stress that those with the disperse phase of SiO_2 synthesized by the sol–gel procedure [63], which is explained by increased external and internal polarization of structurally inhomogeneous particles in the former disperse phase.

The structure of disperse phase material is of decisive importance for the strength of the electrorheological effect. Different electrorheological activities are characteristic of disperse phases both of different materials and of structural modifications of materials belonging to the same natural group. Such differences are associated with quite fine effects.

Shang et al. [64] subjected nanosized titanium dioxide powders (particle sized ~200 nm) obtained by the sol–gel procedure from titanium tetrachloride to thermal treatment at various temperatures and obtained their amorphous (250°C), anatase (350, 450, and 550°C), and mixed rutile–anatase forms (650 and 850°C). The powders were studied as disperse phases of electrorheological fluids in dimethylsilicone oil. The results revealed a dominating role the type of crystal lattice plays in the electrorheological effect. Thus anatase particles exhibited a higher electrorheological activity than rutile-containing, whereas an amorohous titanium dioxide was more active than crystalline. The particle surface area and pore size, as well as the dispersion correlated with the strength of the electrorheological effect. The dynamic yield stress of the electrorheological fluid with an amorphous disperse phase (20%) was about 1.2 kPa at E = 3 kV mm^{-1}.

Yin and Zhao [65] compared the electrorheological efficiencies (at E = 3 kV mm^{-1}) of disperse phases of sodium titanate nanowhiskers with a 1:3.21 Na/Ti ratio (obtained by the hydrothermal procedure in an alkaline medium) and a titanium dioxide powder in the anatase form (average particle size 70–90 nm). Dispersions of TiO_2 nanoparticles (10 vol %) showed low share stresses (80 Pa), whereas the yield stress of nanowhisker dispersions (10 vol %) proved to be 1.1 kPa. Moreover, the latter dispersions showed a higher sedimentation stability.

Electrorheological fluids with the disperse phase on the basis of nanosized powers of a hydroxypropylene cellulose–TiO_2 hybrid organic–inorganic material (particle size 100–300 nm) obtained by the sol–gel procedure [66] showed much higher yield stresses in electric fields higher than 2 kV mm^{-1} compared with the electrorheological fluid on the basis of a nanosized titanium oxide. The dynamic yield stress in electric fields of 4 kV mm^{-1} with a TiO_2 disperse phase (30%) was found to be 0.2 kPa, while with the disperse phase on the basis of the above nanocomposite, 1.3 kPa. It was found that the dispersion of a mixture of the components of the hybrid material shows no synergism of the electrorheological response.

Zhao and Duan [67] made use of in situ sol-gel procedure in an alcohol medium to perform controlled hydrolysis of titanium tetrabutylate, yielding a transpared gel. By introducing in this sol of carboxymethyl starch and polar additives, such as ethylene glycol, citrates, amides, as well as OH- and NH_2-containing surfactants the authors obtained a nanocomposite of TiO_2 with carboxymethyl starch, which was isolated and vacuum-dried. The static yield stress developed by a 39% nanocomposite dispersion in silicone oil was 37 kPa при $E = 4$ kV mm^{-1}, which is several times higher that the yield stresses characteristic of dispersions of the components of this hybrid material. The dispersions showed a high sedimentation stability: The sedimented fraction was 5% after 40 days.

Mesoporous titanium dioxide and mesoporous cerium-doped titanium dioxide (Ce/Ti = 8.5 mol %) were also tested as disperse phases. The materials were synthesized by the sol–gel procedure using tetrabutyltitanate as a precursor and a mixture of octadecylamine and poly(ethylene glycol) (M = 1500) as a template, which gave a wormhole-like mesopore structure. The specific surface area of the material calcined at 450°C was 110 m^2 g^{-1}, pore size 2–3 nm, powder particle size 5000–2000 nm [68]. The static yield stress of the mesoporous TiO_2 dispersion in dimethylsilicone oil (34%) is 8.7 kPa and that of the dispersion of the cerium-doped powder is 14 kPa at $E = 3$ kV mm^{-1}, which is 25 times as high as the static yield stress of the electrorheological fluid on the basis of a usual titanium dioxide and double that for a cerium-doped nonporous titanium dioxide. These results show that mesoporous TiO_2 dispersions show a higher electrorheological activity than those of nonporous TiO_2; combining a mesoporous structure and a cerium doping ensures further strong activity enhancement.

Ma et al. [69] studied electrorheological fluids with nanosized fillers, titanium and zirconium dioxides synthesized by the sol–gel procedure using as dopants rare-earth metal ions (RE=Y, La, Ce, Gd, and Tb; RE/TiO_2 and RE/ZrO_2 molar ratios molar 0.08 and 0.02, respectively) and assessed the effect of microstructure dimensions and filler particle size on the electrorheological activity. It was shown that RE metal ion dopants can either enhance or attenuate the electrorheological activity of materials, depending on grain pore volume. Therewith, a titanium dioxide having a volume-centered lattice and a tetragonal zirconium dioxide induce a stronger electrorheological effect than a tetragonal titanium dioxide and a monoclinic zirconium dioxide. Thus, the filler microstructure and pore volume play an important role in forming the electrorheological effect, and by optimizing the crystal structure and pore volume in nanomaterials one can develop high-performace electrorheological materials. Among known structures, the highest dynamic yield stress (3 kPa at a shift rate of 100 s^{-1} and $E = 4$ kV mm^{-1}) is characteristic of a 25% electrorheological fluid on the basis of titanium dioxide doped with cerium (with a cubic edge-centered lattice) and dimethylsiloxane oil.

Notably, rare-earth metal ion dopants (Y, La, Ce, Gd, and Tb) introduced into the crystal lattice of the nanosized zirconium dioxide prepared by the sol–gel procedure attenuate the electrorheological effect compared with the system on the basis of a pure ZrO_2, the resulting effect depending on the type of the dopant [70]. The observed changes in the electrorheological behavior are explained by the fact that rare-earth metal ions decrease the size of the tetragonal crystal lattice of ZrO_2. Therewith, the dynamic yield stress of a 25% dispersion of zirconium dioxide (powder particle size ~100 nm) in silicone oil is 1.1 kPa at a share rate of 150 s^{-1} and $E = 4$ kV mm^{-1}.

Wu et al. [71] studied the effect of rare-earth metal ion dopants in amorphous titanium dioxide on the activity of the latter as a disperse phase in electrorheological liquids. Materials containing Ba^{2+} and Sr^{2+} separately, as well as a 1:1 Ba^{2+}/Sr^{2+} mixture in a 1:1 RE/Ti molar ratio (sol–gel procedure involving introduction of an RE precursor at the gel formation stage, drying temperature 120°C, powder particle size 50–150 nm). The static yield stresses of 38% dispersions of powders of these materials in dimethylsiloxane oil at a field strength of 3.5 kV mm^{-1} were as follows, kPa: amorphous titanium dioxide 2; для TiO_2 doped with Ba^{2+} 5; TiO_2 doped with Sr^{2+} 8; and TiO_2 doped with Ba^{2+}/Sr^{2+} 15.3. The sedimentation ratio for the electrorheological fluid on the basis of TiO_2+ Ba^{2+}/Sr^{2+} was 99.4% within three months.

An electrorheological fluid with a high yield stress was obtained with a surface-modified strontium titanate [72]. A monodisperse sol of strontium titanate was synthesized by the sol–gel procedure in ethylene glycol. After centrifugation, drying, and calcination the strontium titanate powder was mixed with a suitable surfactant and heated in a vacuum at 80°C for 24 h. The product consisted of single particles or chain aggregates, size range 500–1000 mn. The static yield

stress of a 36% dispersion of this material in silicon oil was 27.2 kPa at E = 3 kV mm^{-1}, which was the top achievement at that time.

Wen and co-workers [73–75] reported on the giant electrorheological effect exhibited by dispersions of barium titanyl oxalate nanoparticles coated with urea {$BaTiO(C_2O_4)_2$ + NH_2CONH_2}. The material was synthesized in the following way. A solution of barium chloride in distilled water, prepared at 50–70°C, was mixed in an ultrasonic bath at 65°C with a solution obtained by adding $TiCl_4$ to an aqueous solution of oxalic acid prepared in an ultrasonic bath at 65°C. This stage gave amorphous nanosized particles of barium titanyl oxalate. A dispersion of these particles in silicon oil showed a maximum static yield stress in electric fields of 5 kPa. Addition of urea to the solution obtained at the first stage gave a white sol which was cooled to room temperature, the precipitate was separated, washed with water, and dried to remove all water to obtain nanoparticles (50–70 nm) formed by the "barium titanyl oxalate–urea shell" type, shell thichkness ~5 nm. The resulting powder was mixed with silicon oil, and the mixture was vigorously stirred and subjected to a vacuum for a few hours to obtain an electrorheological fluid resistant to sedimentation for 5 months. The static yield stress of this fluid (30 % wt/wt disperse phase) was 130 kPa at E = 5 kV mm^{-1}.

The authors associated the appearance of such a giant effect with the overlap of highly polarizable urea shells of disperse phase particles. Therewith, the dense packing of nanosized particles in the dispersion at their high concentrations favor closer interparticle distances sufficient for shell overlap. In the cited works, the barium titanyl oxalate disperse phase was modified with rubidium ions to enhance the polarization contribution. The static yield stress of the electrorheological fluid was 250 kPa at E = 5 kV mm^{-1}.

The static yield stress of a 30% dispersion of a $BaTiO(C_2O_4)_2$ + NH_2CONH_2 powder in a mixture of silicone and hydrocarbon oils is as high as 250 kPa at E = 5 kV mm^{-1}. Addition to the system of a little oleic acid (0.03 vol %) enhances the electrorheological effect [76]: The static yield stress of a 30% dispersion is 260 kPa at E = 3 kV mm^{-1}. The authors of explain this effect by enhanced wetting of disperse phase particles and their distribution ordering.

The high electrorheological activity of oleophilic nanomaterials as the disperse phases of electrorheological fluids was confirmed by Qiao et al. [77]. A titanium dioxide powder was prepared by the sol–gel procedure using sodium dodecyl sulfate (SDS) as an oleophilizing additive for improved oil wettability of the material. The irregular-shaped particles of the organic–inorganic composite were 120 nm in size and contained 1.25% of SDS. The electrorheological fluid prepared from silicon oil and 56 vol % of an SDS powder showed the yield stress of 130 kPa at the electric field strength of 4 kV mm^{-1}.

The possibility of producing electrorheological fluids with high fluidity limits opens up wide perspectives for developing devices implementing the electrorheological effect.

Certain Application Fields of Electrorheological Fluids

Among promising applications of the electrorheological effect and electrorheological fluids we can mention development of recognition devices (for example, a circuit), such as haptic sensor mounted on a robotic finger [78], development of programmed surfaces for haptic sensors [79], as well as development of force displays (plane feedback systems) for interaction with a virtual environment [80] and haptic displays [81]. Force feedback systems called MEMICA (mechanical mirroring using controlled stiffness and actuators) hold great promise [82]. Feedback control mechanisms for aircrats, motor cars, and computer games (force joysticks), looking like a sphere placed in a bowl with an intersurface layer of an electrorheological fluid, are under development [83]. The potential of sliding-mode feedback force control systems is being studied [84].

Electrorheological fluids were used to develop adaptive systems for transport technologies: electrically controlled antiblock brake systems (ABS) [85]; various electrorheological damper systems [86–89]; new types of stepper engines combining the piesoelectrical and electrorheological effects [90]. Devices implementing the electrorheological effect hold promise for developing microdampers and micropumps for microelectromechanic applications [91, 92]. Devices for fixing flexible workpieces on their mechanical processing are being developed [93].

ACKNOWLEDGMENTS

The work was financially supported by the Russian Foundation for Basic Research (project no. 07-03-00300).

REFERENCES

1. US Patent 2417850, 1947.
2. Winslow, W.M., *J. Appl. Phys*., 1949, vol. 20, pp. 1137–1140.
3. Korobko, E.V., *Elektrostrukturirovannye zhidkosti: osobennosti gidromekhaniki i vozmozhnosti ispol'zovaniya* (Electrorheological Fluids: Hydromechanics and Application), Minsk: ITMO AN Belarusi, 1996
4. *Elektroreologicheskii effect* (Electrorheological Effect), Lykova, A.V., Ed., Minsk: Nauka i Tekhnika, 1972.
5. Shul'man, Z.P., Korobko, E.V., and Levin, M.L., *Electroreologicheskie zhidkosti, sostav i osnovnye svoistva* (Electrorheological Fluids), Preprint no. 4 ITMO NANB. Minsk: ITMO NANB, 2001.
6. Derjaguin, B.V., Dukchin, S.S., and Shilov, V.N., *Adv. Colloid Interface Sci*., 1980, vol. 13, pp. 141–150.
7. Trapeznikov, A.A., Petrzhik, G.G., and Chertkova, O.A., *Kolloid. Zh*., 1981, vol. 33, pp. 1134–1137.
8. Block, H. and Kelly, J.P., *J. Phys. D: Appl. Phys*., 1988, vol. 21, p. 1661.
9. Conrad, H., *MRS Bull*., 1998, vol. 23, no. 8, pp. 35–42.
10. Gast, A.P. and Zukoski, C.F., *Adv. Colloid Interface Sci*., 1989, vol. 30, pp. 153–202.
11. Hao, T., *Adv. Mater*., 2001, vol. 13, pp. 1847–1852.
12. Lampe, D., *Materials Database on Commercially Available Electro- and Magnetorheological Fluids (ERF and MRF), http://www.tu-Dresden.de/mwilr/lampe/HAUENG.HTM, updated on 01/30/1997*.
13. Wen, W., Zheng, D.W., and Tu, K.N., *J. Appl. Phys*., 1999, vol. 85, no. 1, pp. 530–533.
14. Deinega, Yu.F. and Vinogradov, G.V., *Rheol. Acta*, 1984, vol. 23, p. 636.
15. GB Patent 2153372, 1985.
16. Wen, W., Huang, X., and Sheng, P., *Soft Matter*., 2008, vol. 4, pp. 200–210.
17. Klass, D.L. and Martinek, T.W., *J. Appl. Phys*., 1967, vol. 38, pp. 67–74.
18. Klass, D.L. and Martinek, T.W., *Ibid*., 1967, vol. 38, pp. 75–80.
19. Weiss, K.D., Carlson, J.D., and Coulter, J.P., *J. Intell. Mater. Sys. Struct*., 1993, vol. 4, pp. 13–34.
20. Block, H. and Kelly J.P., *J. Phys. D.: Appl. Phys*., 1988, vol. 21, p. 1661.
21. Stangroom, J.E., *Phys. Technol*., 1983, vol. 14, pp. 290–296.
22. See, H., Tamura, H., and Doi, M., *J. Phys. D: Appl. Phys*., 1993, vol. 26, pp. 746–752.
23. Tamura, H., See, H., and Doi, M., *Ibid*., 1993, vol. 26, pp. 1181–1187.
24. Kim, Y.D., *J. Colloid Interface Sci*., 2001, vol. 236, pp. 225–232.
25. Kim, Y.D. and Nam, S.W., *Ibid*., 2004, vol. 269, pp. 205–210.
26. Petrzhik, G.G. Chertkova, O.A., and Trapeznikov, A.A., *Dokl. Akad. Nauk SSSR*, 1980, vol. 253, pp. 173–175.
27. Lee, H.J., Chin, B.D., Yang, S.M., and Park, O.O., *J. Colloid Interface Sci*., 1998, vol. 206, pp. 424–438.
28. Kim, J.W., Kim, C.A., Choi, H.J., and Choi, S.B., *Korea–Australia Rheology J*., 2006, vol. 18, no. 1, pp. 25–30.
29. Adriani, P.M. and Gast, A.P., *Phys. Fluids*, 1988, vol. 31, pp. 2757–2768.
30. Klingenberg, D.J., Van Frank, S., and Zukoski, C.F., *J. Chem. Phys*., 1991, vol. 94, pp. 6160–6169.
31. Chen, Y.A., Sprecher, F., and Conrad, H., *J. Appl. Phys*., 1991, vol. 70, pp. 6796–6803.
32. Davis, L.C., *Ibid*., 1992, vol. 72, pp. 1334–1340.
33. Davis, L.C., *Appl. Phys. Lett*., 1992, vol. 60, pp. 319–321.
34. Davis, L.C., *J. Appl. Phys*., 1993, vol. 73, pp. 680–683.
35. Anderson, R.A., *Langmuir*, 1994, vol. 10, pp. 2917–2928.
36. Rankin, P.J. and Klingenberg, D.J., *J. Rheol*., 1998, vol. 42, no. 3, pp. 639–656.
37. Conrad, H. and Wu, C.W., *J. Phys. D: Appl. Phys*., 1997, vol. 30, p. 2634.
38. Klingenberg, D.J., *MRS Bull*., 1998, vol. 23, no. 8, pp. 103–112.
39. Foulc, J.N., Atten, P., and Felici, N., *J. Electrostatics*, 1993, vol. 33, p. 103.
40. Davis, L.C., *J. Appl. Phys*., 1992, vol. 72, no. 4, pp. 1334–1340.
41. Atten, P., Foulc, J.N., and Felici, N., *Int. J. Mod. Phys. B*, 1994, vol. 8, pp. 2731–2745.
42. Wu, C.W. and Conrad, H., *J. Phys. D: Appl. Phys*., 1996, vol. 29, p. 3147.
43. Felici, N., Foulc, J.N., and Atten, P., *Proc. 4th Int. Conf. on ER Fluids Mechanisms*, Singapore: World Scientific, 1994, pp. 139–152.
44. Felici, N.J., *J. Electrostatics*, 1997, vols. 40/41, pp. 567–572.
45. Parthasarathy, M. and Klingenberg, D.G., *Mater. Sci. Eng.,* 1996, vol. 17, pp. 57–103.
46. Wang, X. and Gordaninejad, F., *J. Intel. Mater. Sys. Struct*., 1999, vol. 10, pp. 601–608.
47. Cho, M.S., Choi, H.J., and Chon, M.S., *Polymer,* 2005, vol. 46, p. 11484.
48. Bonnecaze, R.T. and Brady, J.F., *J. Rheol*., 1992, vol. 36, pp. 73–115.
49. Shen, R., Wang, X.Z., Lu,Y., Wen, W.J., Sun, G., and Lu, K.Q., *J. Appl. Phys*., 2007, vol. 102, pp. 024106(3).
50. Kollias A., Dimarogonas D. *J. Intell. Mater. Sys. Struct*., 1993, vol. 4, pp. 519–526.

51. Choi Y.T., Cho J.U., Choi S.B., and Wereley N.M., *Smart Mater. Struct*., 2005, vol. 14, pp. 1025–1036.
52. Kraev, A.S., Agafonov, A.V., Nefedova, T.A., et al., *Izv. Vyssh. Uchebn. Zaved.: Khim. Khim. Tekhnol*., 2007, vol. 50, no. 6, pp. 35–39.
53. US Patent 5445759, 1995.
54. Tao, R., Zhang, X., Tang, X., and Anderson, P., *Phys. Rev. Lett*., 1999, vol. 83, pp. 5575–5578.
55. Choi, H.J., Kim, T.W., Cho, M.S., Kim, S.G. and Jhon, M.S., *Eur. Polym. J*., 1997, vol. 33, pp. 699–703.
56. Goodwin, J.W., Markham, G.M., and Vinent, B., *J. Phys. Chem. B*, 1997, vol. 101, pp. 1961–1967.
57. Cho, M.S., Choi, H.J., and To, K., *Macromol. Rapid Commun*., 1998, vol. 19, pp. 271–273.
58. Kim, S.G., Kim, J.W., Jang, W.H., et al., *Polymer,* 2001, vol. 42, p. 5005.
59. Kim, D-H. and Kim, Y.D., *J. Ind. Eng. Chem*., 2007, vol. 13, no. 6, p. 879.
60. Yoon, D.J. and Kim, Y.D., *J. Colloid Interface Sci*., 2006, vol. 303, pp. 573–578.
61. Yoon, D.J. and Kim, Y.D., *J. Mater. Sci*., 2007, vol. 42, pp. 5534–5538.
62. Fang, F.F. and Choi, H.J., *J. Ind. Eng. Chem*., 2006, vol. 12, no. 6, pp. 843–845.
63. Nefedova, T.A., Agafonov A.V., et al., *Mekh. Kompoz. Mater.Konstrukts*., 2006, vol. 12, no. 3, pp. 391–406.
64. Shang, Y., Ma, S., Li, J., Li, M., Wang, J., and Zhang, S., *J. Mater. Sci. Technol*., 2006, vol. 22, no. 4, pp. 572–576.
65. Yin, J. and Zhao, X., *Nanotechnology*, 2006, vol. 17, pp. 192–196.
66. Kraev, A.S., Agafonov, A.V., Davydova, O.I., et al*., Kolloid. Zh*., 2007, vol. 69, no. 5, pp. 661–667.
67. Zhao, X.P. and Duan, X., *Mater. Lett*., 2002, vol. 54, pp. 348–351.
68. Yin, Y. and Zhao, X.J., *Mater. Chem*., 2003, vol. 13, pp. 689–695.
69. Ma, S.Z., Liao, F.H., Li, S.X., Xu, M.Y., Li, J.R., Zhang, S.H., Chen, S.M., Huang, R.L., and Gao, S., *Ibid*., 2003, vol. 13, pp. 3096–3102.
70. Liao, F.H., Zhang, L., Li, J-R., Xu, G., Li, G-B., Zhang, S.H., and Gao, S., *J. Solid State Chem*., 2003, vol. 176, pp. 273–278.
71. Wu, Q., Zhao, B.Y., Chen, L.S., and Hu, K.A., *Scr. Mater*., 2004, vol. 50, pp. 635–639.
72. Zhang, Y., Lu, K., Rao, G., Tian, Y., Zhang, S., and Liang, J., *Appl. Phys. Lett*., 2002, vol. 80, no. 5, pp. 888–890.
73. Wen, W., Huang, X., Yang, S., Lu, K., and Sheng, P., *Nature Materials*, 2003, no. 2, pp. 727.
74. Huang, X., Wen, W., Yang, S., and Sheng, P., *Solid State Commun*., 2006, vol. 139, pp. 581–588.
75. Gong, X., Wu, J., Huang, X., Wen, W., and Sheng, P., *Nanotechnology,* 2008, vol. 19, p. 165602(7).
76. Shen, C., Wen, W., Yang, S., andd Sheng, P., *J. Appl. Phys*., 2006, vol. 99, p. 106104(3).
77. Qiao, Y., Yin, J., and Zhao, X., *Smart Mater. Struct*., 2007, vol. 16, p. 332.
78. Kenaley, G.L. and Cutkosky, M.R., *Proc. IEEE Int. Conf. on Robotics and Automation*, Scottsdale, AR, 1989, pp. 132–136.
79. Taylor, P.M., Hosseini-Sianaki, A., and Varley, C.J., *Int. J. Mod. Phys. B*, 1996, vol. 10, p. 3011.
80. Sakaguchi, M. and Furusho, J., *Proc. IEEE Int.Conf. on Robotics and Automation*, Leuven, Belgium, 1998, pp. 2586–2590.
81. Liu, Y., Davidson, R., and Taylor, P., *Smart Mater. Struct*., 2005, vol. 14, pp. 1563–1568.
82. Mavroidis, C, Pfeiffer, C., Celestino, J., and Bar-Cohen, Y., *Proc. ASME Mechanisms and Robotics Conf*., Baltimore, MD, 2000, p. DETC2000/MECH-14121.
83. Böse, H., Berkemeier, J., and Trendler, A., *Proc. ACTUATOR Conf.,* Bremen, Germany, 2000, pp. 563–566.
84. Han, Y-M. and Choi, S-B., *Smart Mater. Struct*., 2006, vol. 15, p. 1438.
85. Choi, S.B., Lee, T.H., Lee, Y.S., and Han, M.S., *Ibid*., 2005, vol. 14, p. 1483.
86. Bitman, L., Choi, Y.T., et al., *Ibid*., 2005, vol. 14, pp. 237–246.
87. Chonan, S., Tanaka, M., et al., *Ibid*., 2004, vol. 13, pp. 1195–1202.
88. Wereley, N.M., Lindler, J., Rosenfeld, N., and Choi, Y-T., *Ibid*., 2004, vol. 13, pp. 743–752.
89. Nikolaev, Yu.I., Binshtok, A.E., Efremov, V.L., Korobko, E.V., Levin, M.L., and Bilyk, V.A., *Avtomob. Prom-st',* 2005, no. 11, pp. 19–22.
90. Chu, X., Qiu, H., Li, L., and Gui, Z., *Smart Mater. Struct*., 2004, vol. 13, pp. N51–N56.
91. Niu, X., Liu, L., Wen, W., and Sheng, P., *Phys. Rev. Lett*., 2006, vol. 97, p. 044501.
92. Liu, L., Niu, X., Wen, W., and Sheng, P., *Appl. Phys. Lett*., 2006, vol. 88, p. 173505.
93. Korobko, E.V., Bilyk, V.A., Korobko, O.A., Mardosevich, M.I., Basinyuk, V.A., and Mardosevich, E.I., *Vestn. Polotsk. Gos. Univ., Ser. V*, 2005, no. 12, pp. 94–97.